Preparation of MnS-FeOCl composite and its Fenton-like reaction performance under different pH

Yaoji Chen[a], Guoping Zhao[a], Yuan Shi[a], Ziyi Zhang[b], Jie Wang[b], Shaoping Tong[b],*

[a]_Zhejiang Tiandi Environmental Protection Technology Co., Ltd., Hangzhou 311121; emails: 178540408@qq.com (Y. Chen), 8803591@qq.com (G. Zhao), shiyuan515@163.com (Y. Shi)_
[b]_College of Chemical Engineering, State Key Laboratory Breeding Base of Green Chemistry-Synthesis Technology, Zhejiang University of Technology, Hangzhou, Zhejiang 310014, China, emails: sptong@zjut.edu.cn (S. Tong), 211122010211@zjut.edu.cn (Z. Zhang), 13966384235@163.com (J. Wang)_

ABSTRACT

A composite of manganese sulfide doped iron oxychloride (MnS-FeOCl) was successfully synthesized for the first time and applied to activate H_2O_2 to degrade isoniazid under different pH values. The MnS-FeOCl structure was characterized by various analytical methods such as X-ray diffraction (XRD), scanning electron microscopy, energy-dispersive X-ray spectroscopy, Fourier-transform infrared spectroscopy and X-ray photoelectron spectroscopy, indicating manganese sulfide (MnS) doping greatly changed the physicochemical property of FeOCl. The Fenton-like reaction showed that MnS doping could enhance the Fenton activity of FeOCl in the pH range of 6–9, and 5% MnS-FeOCl composite had the highest activity. Isoniazid (20 mg/L) could be degraded by 89.90% in 5 min at an initial pH of 6.0 by 5% MnS-FeOCl/H_2O_2. However, the high performance of 5% MnS-FeOCl composite was at the cost of decrease of its stability. The result of XRD analysis indicated that the crystallinity of 5% MnS-FeOCl was poorer than that of pristine FeOCl, thus leading to its decreased stability. It is of great significance for the further study on the modification of FeOCl catalyst in Fenton-like reaction.

Keywords: Iron oxychloride; Manganese sulfide; Fenton-like; Isoniazid; Degradation

1. Introduction

The presence of biodegradable substances in pharmaceutical wastewater makes conventional treatment methods ineffective, and the residual antibiotics in the water can cause serious environmental and health problems [1,2]. For example, isoniazid (INH), as an anti-tuberculosis drug, is often detected in environmental water. Although the antibacterial and bactericidal effect of INH is significant, its side effect, like damage to the nervous system and liver is also relatively large, implying INH in water will possibly pose ecological risks [3,4]. Various water purification technologies including physical, chemical and biological techniques have been developed to solve this problem [5,6], and Fenton reaction is the promising one among them. Compared with homogeneous Fenton reaction, heterogeneous Fenton reaction technology has attracted more attention owing to easy recovery of catalyst [7–9]. However, suitable catalyst in heterogeneous Fenton-like reaction under the neutral conditions is still at the state of shortage.

FeOCl has good catalytic performance in Fenton-like reaction under neutral conditions [10–12]. Recently, method of doping or combining has gained much attention to further improve the Fenton activity of FeOCl [13–15]. There are many reports about the successful improvement of FeOCl catalytic activity by metal doping [16,17]. For example,

* Corresponding author.

Ln-FeOCl generated new catalytic active centers compared with pristine FeOCl [18], and then had higher catalytic activity. Sn-FeOCl increased the specific surface area and the number of active sites [19], thus promoting the decomposition of H_2O_2 to generate hydroxyl radicals for the degradation of organic compounds. The studies about the combining a compound or doping a non-metal element with FeOCl are also gradually increasing. Qu et al. [20] found that the catalyst performance of FeOCl could be dramatically improved by combining with MoS_2, and 95.8% methylene blue could be removed within 2 min at pH 5.8. Lu et al. [21] prepared C-doped FeOCl, and found that the C-doping increased the content of Fe^{2+} (11.3% to 40.4%), and 99% of tetracycline hydrochloride could be degraded within 6 min.

Although the method of doping or combining is beneficial to the Fenton activity of FeOCl, it always accompanies a decrease in its stability. Jinsheng et al. [22] prepared Cu-FeOCl and found its stability decreased gradually with increasing Cu(II) content. The Ag-doped FeOCl showed similar results [23]. However, these reports did not specifically study the reason why the doped FeOCl was more prone to be deactivation. The manganese sulfide doped iron oxychloride (MnS-FeOCl) composite was successfully prepared in this work for the first time, and its Fenton activity and stability were investigated in detail. The physicochemical property of MnS-FeOCl was characterized by X-ray diffraction (XRD), scanning electron microscopy (SEM), X-ray photoelectron spectroscopy (XPS) and Fourier-transform infrared spectroscopy (FTIR). It was found that the way of manganese sulfide (MnS) doping could enhance the ratio of Fe(II) to Fe(III) and the amount of OH group but reduce the crystallinity of FeOCl, thus resulting in its enhanced Fenton activity and decreased stability. The results of this study can possibly provide a thought for the rational design of FeOCl with high Fenton activity and stability to solve the environmental pollutant problem.

2. Experimental set-up

2.1. Materials and reagents

Ferric chloride hexahydrate ($FeCl_3 \cdot 6H_2O$), MnS, sodium hydroxide (NaOH), sulfuric acid (H_2SO_4), INH, ammonium acetate (CH_3COONH_4), *tert*-butanol (TBA), sodium azide (NaN_3), *p*-benzoquinone (PBQ) and acetone (C_3H_6O) were analytical grade, methanol (CH_3OH) was chromatographic grade, hydrogen peroxide (H_2O_2) concentration was 30%. All chemicals were purchased from Sinopharm Chemical Reagent Co., Ltd., (Shanghai, China). Deionized water was used throughout this study.

2.2. Characterization

X-ray powder diffraction (XRD, Rigaku, SmartLab SE, Japan) was used to determine the crystal structures. X-ray photoelectron spectroscopy (XPS, Kratos AXIS Ultra DLD, UK) was conducted to analyze the elemental composition and chemical state. Gemini 500 high-resolution transmission electron microscopy (Carl Zeiss, Germany) was used to detect the morphology of the catalyst. The concentration of isoniazid was analyzed by a high-performance liquid chromatography (HPLC, Thermo Fisher Technology (China) Co.,

Ltd., Dionex UltiMate 3000). The column was C18, and the ultraviolet absorption wavelength was 263 nm. The mobile phase was a mixture of methanol and 5 mmol/L ammonium acetate in a volume ratio of 1:9, and the flow rate was 0.8 mL/min.

2.3. Preparation of the catalyst

2.3.1. Synthesis of the catalyst

Taking 2.0 g $FeCl_3 \cdot 6H_2O$ with appropriate amount of MnS (0.04, 0.1, 0.2, and 0.4 g) into a glass beaker with 10 mL deionized water, the mixture was sonicated for 30 min and then stirred magnetically at 80°C for 8 min to obtain a well-mixed solid substance. The obtained solid was heated in a muffle furnace under air atmosphere at a rate of 5°C/min to 230°C for 150 min. After cooling to room temperature, the sample was ground into powders. The MnS-FeOCl composites with different mass percentages of MnS (2%, 5%, 10% and 20%) were prepared and correspondingly labeled as 2% MnS-FeOCl, 5% MnS-FeOCl, 10% MnS-FeOCl, and 20% MnS-FeOCl. Pure FeOCl was also prepared by a similar method without MnS.

2.3.2. Fenton-like performance evaluation

The degradation experiment was carried out in a 250 mL beaker unless otherwise specified. Typical experimental procedure for degradation of INH by MnS-FeOCl/H_2O_2 system was as follows: 200 mL of 10 mg/L INH solution was adjusted to the wanted pH (initial pH) with 1.0 mol/L H_2SO_4 solution or 2.0 mol/L NaOH solution with a magnetic bar at a speed of 600 rpm, then 0.04 g catalyst and 4.0 mg H_2O_2 were added to the solution to trigger degradation of INH. The sample (1 mL) was extracted out at regular intervals, and filtered through 0.22 μm syringe filters for HPLC analysis. The adsorption experiment was performed under similar conditions without H_2O_2.

All experiments were conducted thrice and the average value of the results was recorded. After the reaction, the used catalyst was recovered by suction filtration, washed with deionized water, dried at 60°C for 1.5 h, and then used in the next cycle to evaluate its stability.

3. Results and discussion

3.1. Catalyst characterization

The XRD spectra of MnS-FeOCl composites with different mass percentages of MnS are shown in Fig. 1. The prepared MnS-FeOCl composites and FeOCl are well matched with FeOCl (PDF#24-1005). Compared with that of FeOCl, the half-peak width of the main peak (101) of MnS-FeOCl increases, especially for 5% MnS-FeOCl. In addition, the diffraction intensities of the main peak (110) of the different MnS-FeOCl composites all decrease, indicating the crystallinity of MnS-FeOCl composite reduces. Meanwhile, the position of the diffraction peak (110) of 5% MnS-FeOCl weakly shifts towards lower value, which may be due to the replacement of Fe by Mn with a larger radius [24,25]. Due to the low content and uniform distribution of MnS in the composites, no MnS diffraction peak is observed (Fig. 1). When the mass percentage of MnS increased to 20%
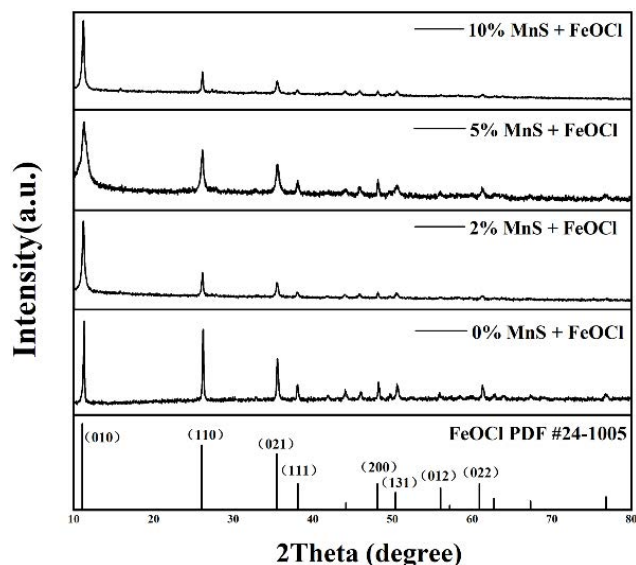
Fig. 1. X-ray diffraction of MnS-FeOCl with different mass percentages of MnS.

(Fig. S1), the XRD pattern of 20% MnS-FeOCl appeared diffraction peaks of the crystal planes (–110), (020), and (111) of $FeCl_2$ at 15.97°, 20.67°, 30.99° (PDF#25-1040), and the crystal planes (200), (220) of MnS at 34.33°, 49.32° (PDF#88-2223), respectively [11]. It can be concluded that too much percentage of MnS will results in different phase composition of MnS-FeOCl composite.

The XPS spectra of FeOCl and 5% MnS-FeOCl are shown in Fig. 2. The peaks around 709 and 722 eV correspond to the characteristic peak of Fe2p in the 5% MnS-FeOCl composites. It is noteworthy that the Fe2p binding energy of 5% MnS-FeOCl in Fig. 2b slightly decreases by 1.67 eV. This phenomenon may be attributed to the change in electron cloud density of Fe due to the partial substitution of Mn for Fe [26]. The O binding energy of 5% MnS-FeOCl in Fig. 2c is divided into 531.72 and 529.72 eV, corresponding to hydroxyl oxygen (O–H) and metallic oxygen (M–O), respectively [27]. The O–H content in 5% MnS-FeOCl is calculated to be 19.03%, which is consistent with the results of FTIR analysis (Fig. S2). As shown in Fig. 2d, the two strong peaks at 197.84 and 199.49 eV belong to Cl2p of Fe–Cl with different coordination numbers, respectively [26], and the introduction of MnS reduces its binding energy [28]. The binding energies of S at 163 and 170 eV in Fig. 2e correspond to Mn–S and Fe–S, respectively. The binding energies of Mn at 641 and 653 eV correspond to Mn2p in Mn–S and Mn–O, respectively. The results confirm the successful doping of FeOCl with MnS [29].

As shown in Fig. 3a, the aggregation of lamellar with a size of about 200–300 nm can be observed with visible interlayer interfaces. In addition, a spherical morphology can also be found in the SEM image of 5% MnS-FeOCl composites, which should be spherical MnS (Fig. 3b). The lattice stripe (0.308 nm) in Fig. 3c corresponding to the (111) crystallographic feature of MnS (PDF#88-2223). The lattice stripes (0.187 and 0.182 nm) in Fig. 3d correspond to the (200) crystallographic feature of FeOCl (PDF#24-1005), where MnS

doping slightly reduces the FeOCl (200) crystallographic distance. The energy-dispersive X-ray spectroscopy (EDS) of the 5% MnS-FeOCl composites was analyzed. As shown in Fig. 4 and Fig. S3, the EDS results show a uniform distribution of Mn, S, Fe, O, and Cl with mass ratios of 2.17%, 0.57%, 55.11%, 20.10%, and 22.05%, respectively, which are close to the theoretical values.

3.2. Effect of reaction parameters on the removal of isoniazid

3.2.1. Effect of different mass percentages of MnS

The effect of different mass percentages of MnS in MnS-FeOCl composites on the degradation of INH by H_2O_2 was investigated. As shown in Fig. 5, the removal of INH by 2%, 5% and 10% MnS-FeOCl/H_2O_2 are 58.53%, 89.90% and 44.84%, respectively, all higher than those of FeOCl/H_2O_2 (32.99%) and MnS/H_2O_2 (40.65%), indicating that the MnS doping has a facilitating effect on the activity of FeOCl in Fenton-like reaction. Moreover, the removal of INH by mechanically mixed MnS-FeOCl (5%/95%, mass ratio)/H_2O_2 was found to be 48.00% within 5 min, which was much lower than that by 5% MnS-FeOCl/H_2O_2 (89.90%), indicating that only mechanically mixing of MnS had limited effect on the Fenton activity of FeOCl in this process.

3.2.2. Effect of initial pH

FeOCl has good catalytic performance at neutral pH [10]. The effect of the initial pH values of 5.0, 6.0, 7.0, 8.0 and 9.0 on the degradation of INH by 5% MnS-FeOCl/H_2O_2 were evaluated (Fig. 6). As shown in Fig. 6, the removal rates of INH after 5 min of reaction are 99.68%, 89.90%, 48.75%, 38.93% and 30.24% at the initial pH values of 5.0, 6.0, 7.0, 8.0 and 9.0, respectively, which is similar to the result of pristine FeOCl. However, 5% MnS-FeOCl composite has higher Fenton-like activity under neutral conditions than pristine FeOCl, and can effectively remove INH in a shorter time with lower H_2O_2 dosage. The pH_{pzc} (pH at which the charge on the surface of the catalyst is zero) of 5% MnS-FeOCl composites was measured to be 1.85 using the salt addition method (Fig. S4), which is similar to that of pristine FeOCl. That is to say, adding 5% MnS-FeOCl to solution also can rapidly change the pH of the solution, then enhancing the efficiency of 5% MnS-FeOCl/H_2O_2.

The universality of 5% MnS-FeOCl/H_2O_2 was also tested in degradation of other organic like p-aminobenzoic acid (PABA), and nicotinamide (NAM). As shown in Fig. S5, the degradation efficiencies of PABA and NAM are 63.04% and 87.53% within 5 min at the initial pH of 6.0, respectively. The results show that the oxidative efficiency of 5% MnS-FeOCl/H_2O_2 is relatively universal in the degradation of other organic pollutants.

3.3. Stability study of 5% MnS-FeOCl and its mechanism

3.3.1. Stability of 5% MnS-FeOCl at different initial pH

To evaluate the application of 5% MnS-FeOCl, the stability of 5% MnS-FeOCl composites at different initial pH was investigated. As shown in Fig. 7, when the initial pH values are 5.0, 6.0, 7.0, 8.0, and 9.0, the removal rates
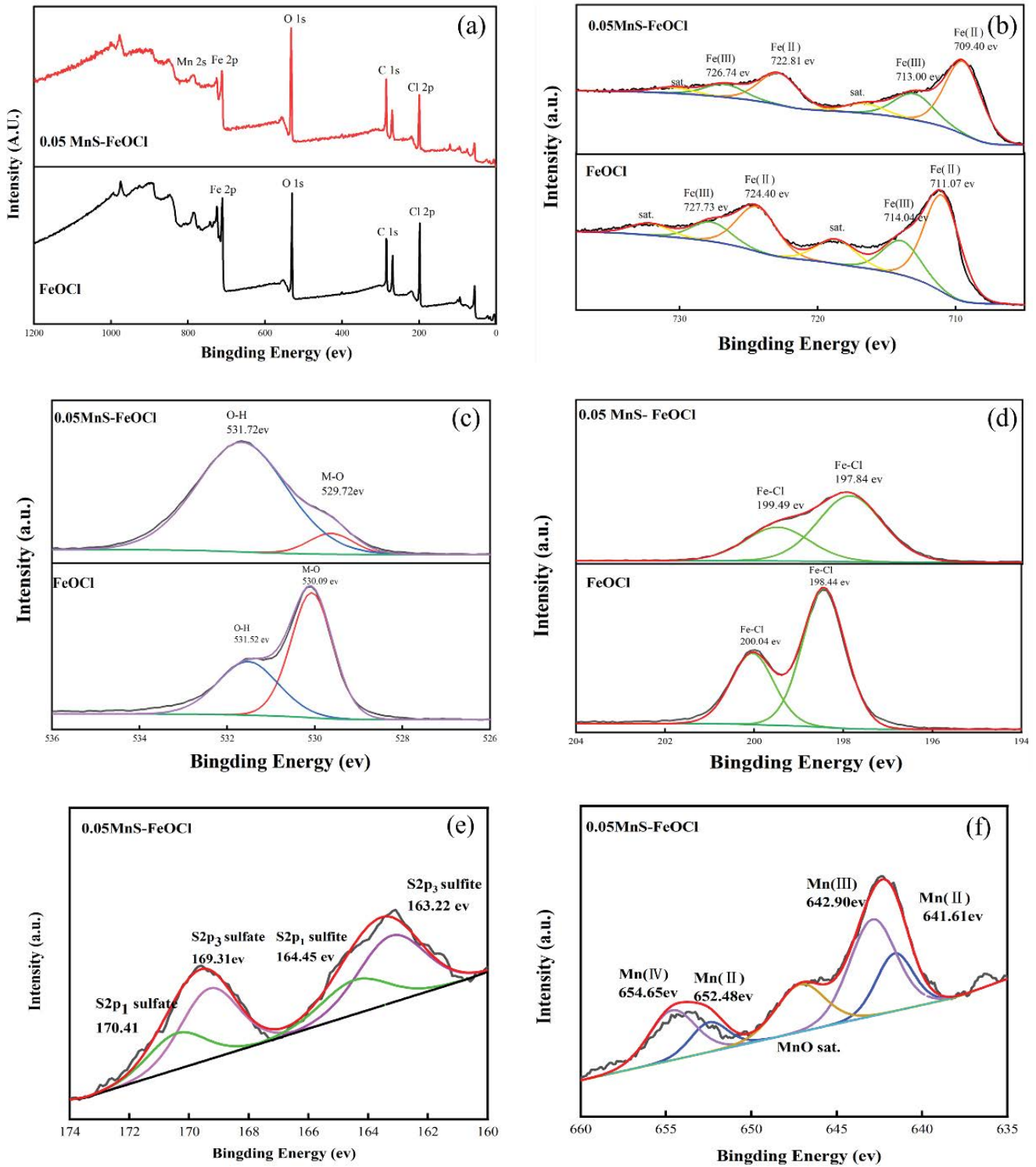
Fig. 2. X-ray photoelectron spectroscopy of 5% MnS-FeOCl.

of INH decrease by 80.86%, 36.52%, 19.30%, 18.59%, and 15.69% within 5 min after three consecutive cycles, respectively. The results show that the decreasing trend of INH removal rate tends to slow down with the increase of initial pH, indicating that the stability of 5% MnS-FeOCl is relatively good under neutral or base conditions. Compared with FeOCl (the removal rate of INH decreased by only 6.32% after four consecutive cycles [30]), 5% MnS-FeOCl is less stable at the initial pH 6.0. Therefore, it is really necessary to further study the reason why 5% MnS-FeOCl deactivates more fast than pristine FeOCl under the similar conditions.
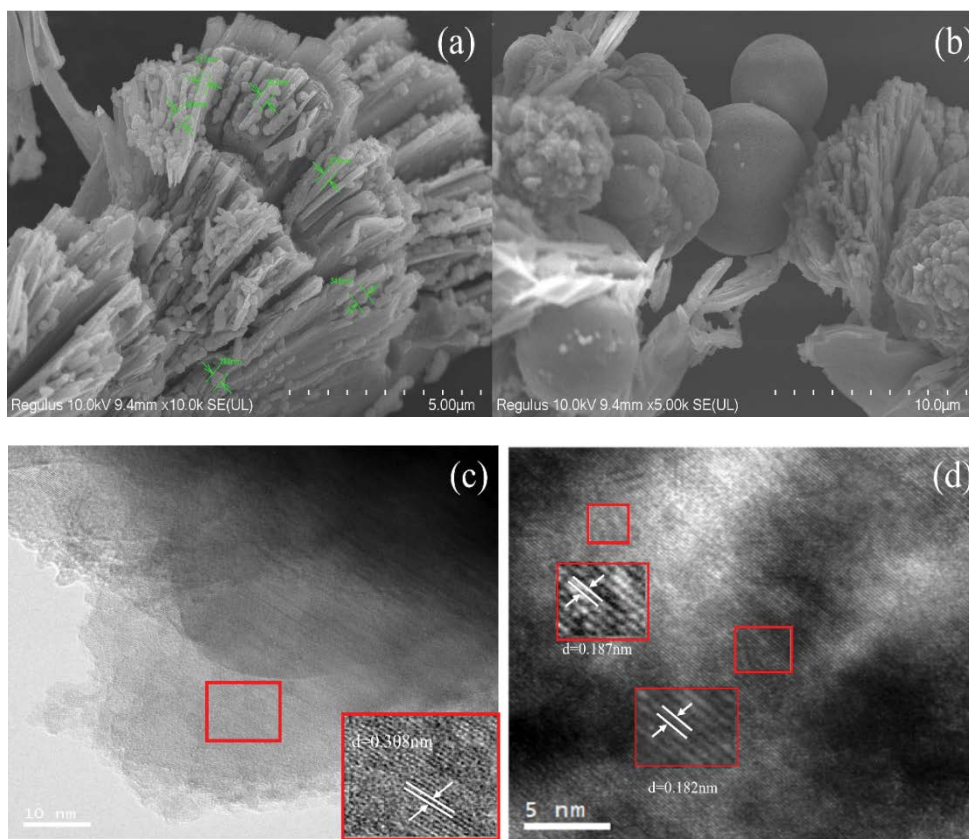
Fig. 3. Scanning electron microscopy of 5% MnS-FeOCl (a,b) and transmission electron microscopy of 5% MnS-FeOCl (c,d).

3.3.2. Mechanism of 5% MnS-FeOCl deactivation

Although the MnS doping can effectively improve the catalytic activity of FeOCl, its stability has an unacceptable decrease. According to our previous study on the stability of FeOCl, three reasons can be used to explain the deactivation of 5% MnS-FeOCl: (1) phase transfer from FeOCl to other iron oxides, (2) the weakened pH regulatory capacity of the used 5% MnS-FeOCl, and (3) dissolution of Fe [30]. Therefore, the XRD patterns of fresh and used 5% MnS-FeOCl were analyzed and shown in Fig. 8. After three consecutive cycles, besides the main diffraction peaks of FeOCl, the used 5% MnS-FeOCl also appears some diffraction peaks of Fe_2O_3 (PDF#72-0469) with 2θ = 24.02°, 33.06°, and 40.74°, which correspond to its (012), (104), and (113) crystal planes, respectively. This result is different with that of used pristine FeOCl (no new diffraction peak was observed after three recycling tests), meaning the formation of Fe_2O_3 may be one reason for fast deactivation of 5% MnS-FeOCl.

The acidifying ability of 5% MnS-FeOCl is another important factor for the degradation of organic matter at neutral pH. The change of solution pH during the cyclic reactions were monitored at an initial pH of 6.0, and the pH_{final} of 3.5, 4.2, and 4.8 were observed in three reuses, respectively. The result indicates the acidification ability of 5% MnS-FeOCl is similar to that of pristine FeOCl, indicating the weakened pH acidifying ability of 5% MnS-FeOCl is not the reason for its fast deactivation.

Under the conditions of 0.1 g/L 5% MnS-FeOCl and initial pH 6.0, the dissolved Fe ion and Mn ion concentrations of 5% MnS-FeOCl composite were analyzed to be 4.1 and 0.66 mg/L, respectively. The dissolved iron ion concentration of 5% MnS-FeOCl is about 2.7 times of that of pristine FeOCl (1.5 mg/L) [30], which may be the other factor for its fast deactivation. Therefore, although MnS doping makes 5% MnS-FeOCl composites higher activity, more Fe ion will be dissolved, then leading to a decrease in its stability. The result is also reported by some similar studies on the Fenton activity of doped FeOCl (Table 1). Chen et al. [31] prepared Sb-FeOCl for the degradation of glutathione, and the XRD result of nanorod-like Sb-FeOCl showed the FeOCl diffraction peaks were broadened with a lower stability. Dingsheng et al. [32] prepared WS-FeOCl and found that the main crystalline plane (110) of FeOCl had a significant decrease in intensity in spite of no new phase formation in the doped FeOCl.

On the basis of above discussion, one can conclude that both phase transformation from FeOCl to Fe_2O_3 and fast dissolution of Fe ion may be two factors for the decreased stability of MnS-FeOCl composites. The increase in Fenton activity of FeOCl by MnS doping is at the cost of reducing its stability, which is also confirmed by some relative literatures. That is to say, the introduction of transition metal can always effectively improve the Fenton activity of FeOCl, but the crystallinity and stability of modified FeOCl always decrease. Therefore, how to obtain a suitable crystallinity
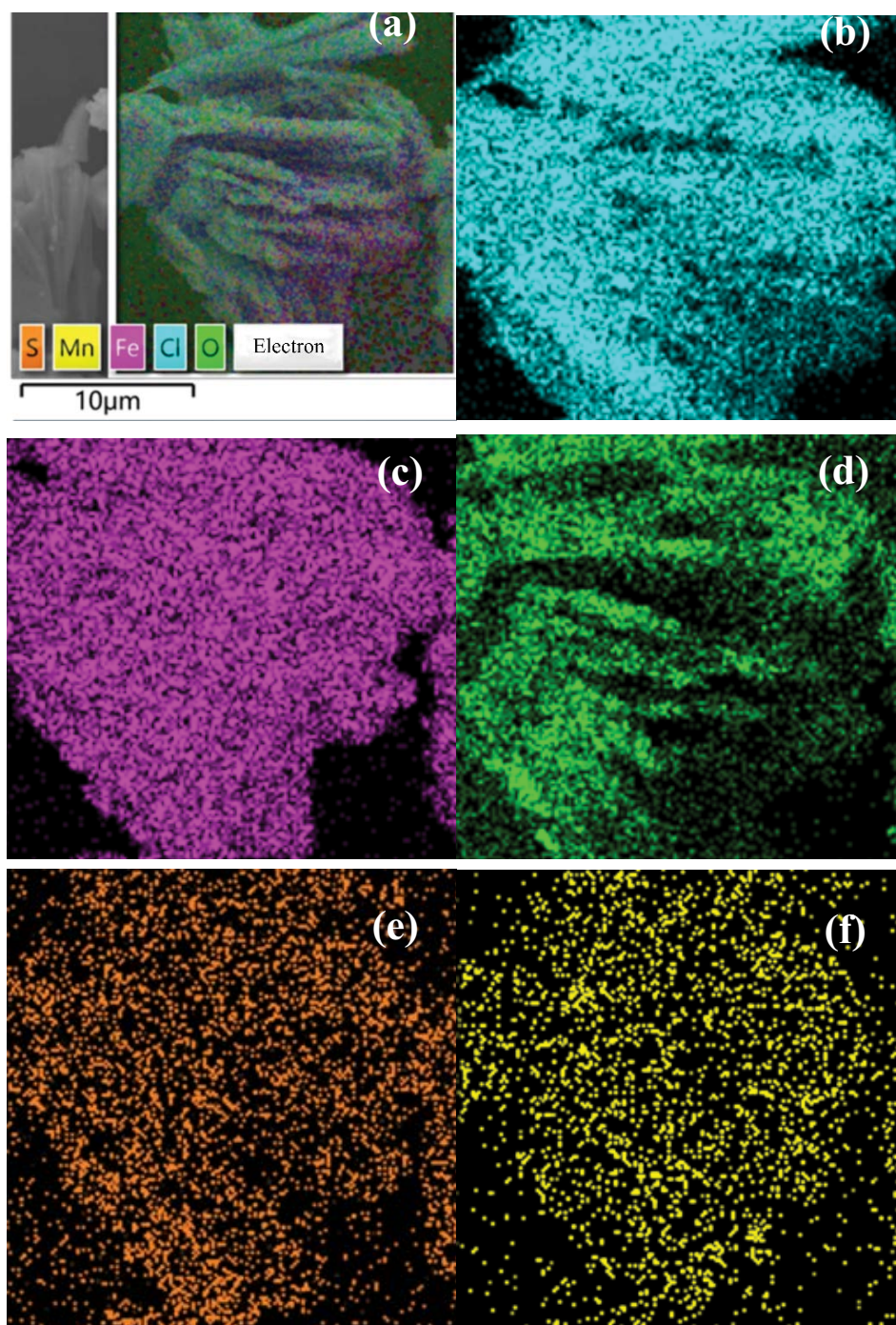
Fig. 4. 5% MnS-FeOCl energy-dispersive X-ray spectroscopy element mapping image (a), Cl (b), Fe (c), O (d), S (e) and Mn (f).

of modified FeOCl with both high Fenton activity and stability are the focus of FeOCl preparation in the future.

4. Conclusion

Different mass fractions of MnS doped FeOCl composites were prepared, and 5% MnS-FeOCl composites was proved to have the highest Fenton activity in the degradation of isoniazid. The physicochemical property of the 5% MnS-FeOCl composites was characterized by XRD, SEM, EDS, FTIR, XPS. It was found that the MnS doping could enhance the ratio of Fe(II) to Fe(III) and the amount of OH group. INH degradation test showed that MnS doping could effectively improve the Fenton activity of FeOCl, the removal rate of 20 mg/L INH reached 89.90% in 5 min at an initial pH 6.0 by 5% MnS-FeOCl/H_2O_2, which was far outperformed those by FeOCl/H_2O_2 and MnS/H_2O_2. However, MnS doping led to a decreased crystallinity of FeOCl, thus decreasing
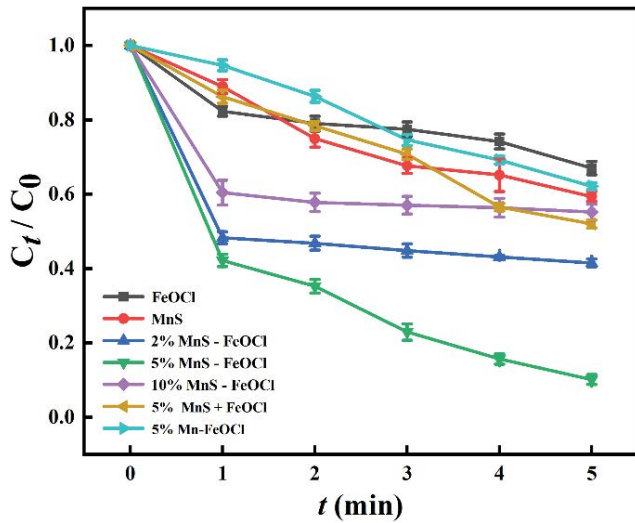
Fig. 5. Effect of different mass percent of MnS in MnS-FeOCl on degradation of isoniazid. Reaction conditions: temperature: 25°C, catalyst dosage: 0.1 g/L, INH concentration: 20 mg/L, H_2O_2 concentration: 10 mg/L, initial pH: 6.0.
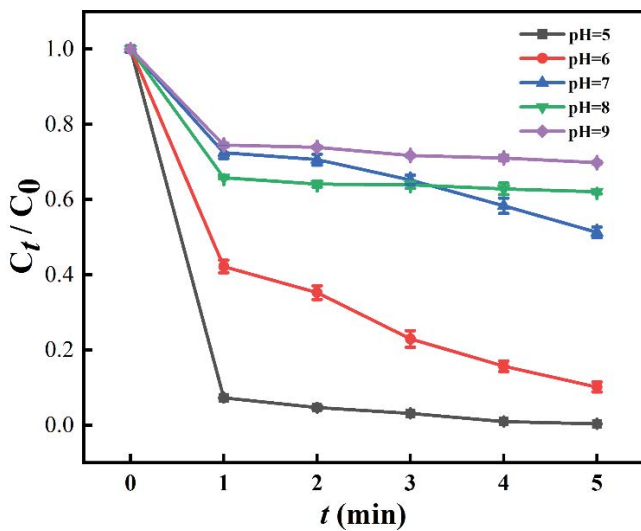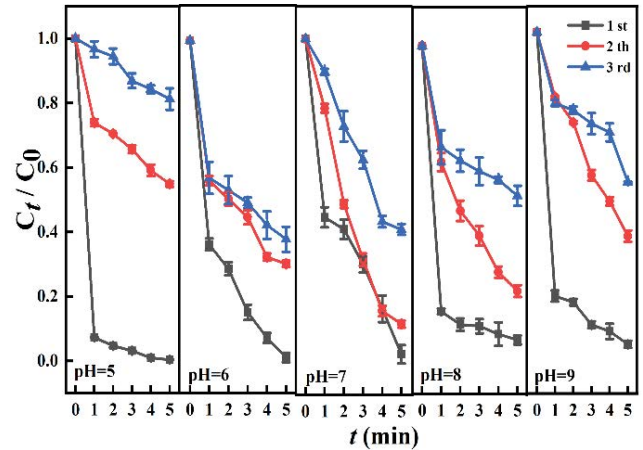

Fig. 7. Stability of 5% MnS-FeOCl at different initial pH. Reaction conditions: temperature: 25°C, catalyst dosage: 0.1 g/L, INH concentration: 20 mg/L, H_2O_2 concentration: 10 mg/L, initial pH: 5.0, 6.0, 7.0, 8.0, and 9.0.

Fig. 6. Effect of different initial pH on the degradation of INH by 5% MnS-FeOCl/H_2O_2. Reaction conditions: temperature: 25°C, catalyst dosage: 0.1 g/L, INH concentration: 20 mg/L, H_2O_2 concentration: 10 mg/L.
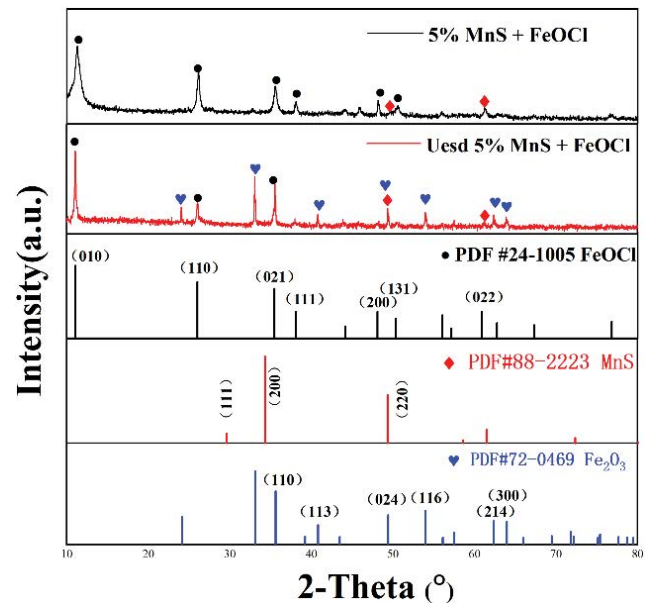

Fig. 8. X-ray diffraction of 5% MnS-FeOCl before and after the reaction at initial pH 6.0.

Table 1
X-ray diffraction of different metal-doped FeOCl

Catalyst	X-ray diffraction
Cu-FeOCl [22]	The main peak (010) and diffraction peak (120) decrease gradually with increasing Cu(II) content
MoS$_2$-FeOCl [33]	Due to the doping of S and Mo atoms into the FeOCl lattice, the diffraction peaks of doped FeOCl slightly decrease compared to those of pristine FeOCl
WS-FeOCl [32]	The peaks of (010) and (110) have a significant decrease in intensity
Ag-FeOCl [23]	The (010) and (110) reflection peaks of Ag-Fe are broadened, and the intensity is significantly low
Ce-FeOCl [34]	Slightly reduced angle of the diffraction peaks of CeOx/FeOCl compared to that of FeOCl

its stability in the Fenton-like reaction. Both phase transformation from $FeOCl$ to Fe_2O_3 and fast dissolution of Fe ion are the two factors for fast deactivation of 5% MnS-FeOCl.

Declaration of competing interest

The authors declare that they have no known competing financial interests or personal relationships that could have appeared to influence the work reported in this paper.

References

[1] X. Liu, T. Tan, Y. Bai, L. Chou, Restoration performance of regional soil and water resources in China based on index of coupling and improved assessment tool, Alexandria Eng. J., 61 (2021) 5677–5686.

[2] M. Pirsaheb, H. Mohamadisorkali, H. Hossaini, H. Hossini, P. Makhdoumi, The hybrid system successfully to consisting of activated sludge and biofilter process from hospital wastewater: ecotoxicological study, J. Environ. Manage. 276 (2020) 111098, doi: 10.1016/j.jenvman.2020.111098.

[3] I. Metushi, J. Uetrecht, E. Phillips, Mechanism of isoniazid-induced hepatotoxicity: then and now, Br. J. Clin. Pharmacol., 81 (2016) 1030–1036.

[4] E.A. Santos, J.C. Saraiva Gonçalves, M.K. Fleury, A.L. Kritski, M.M. Oliveira, L.S. Velasque, J.R. Lapae E Silva, R. de Cássia E Estrela, Relationship of anti-tuberculosis drug-induced liver injury and genetic polymorphisms in CYP_2E_1 and GST, Braz. J. Infect. Dis., 23 (2019) 381–387.

[5] S. Marwa, M.M. Mohamed, A.M. Munjed, A.H. Mohamed, H. Ashraf Aly, A. Jafar, J. Jinho, A critical review of the recent developments in micro–nano bubbles applications for domestic and industrial wastewater treatment, Alexandria Eng. J., 61 (2022) 6591–6612.

[6] R.R. Nair, P. Demarche, S.N. Agathos, Formulation and characterization of an immobilized laccase biocatalyst and its application to eliminate organic micropollutants in wastewater, New Biotechnol., 30 (2013) 814–823.

[7] H. Sun, D. Ren, R. Kong, D. Wang, H. Jiang, J. Tan, D. Wu, S. Chen, B. Shen, Tuning 1-hexene/n-hexane adsorption on MOF-74 *via* constructing Co-Mg bimetallic frameworks, Microporous Mesoporous Mater., 284 (2019) 151–160.

[8] J. Pratiwi, J.-Y. Lin, N.N.N. Mahasti, Y.-J. Shih, Y.-H. Huang, Fluidized-bed synthesis of iron-copper bimetallic catalyst ($Fe^{III}Cu^I@SiO_2$) for mineralization of benzoic acid in blue light-assisted Fenton process, J. Taiwan Inst. Chem. Eng., 119 (2021) 60–69.

[9] T. Sun, M. Gong, Y. Cai, S. Xiao, L. Zhang, Y. Zhang, Z. Xu, D. Zhang, Y. Liu, C. Zhou, MCM-41-supported Fe(Mn)/Cu bimetallic heterogeneous catalysis for enhanced and recyclable photo-Fenton degradation of methylene blue, Res. Chem. Intermed., 46 (2019) 459–474.

[10] S. Asadzadeh-Khaneghah, A. Habibi-Yangjeh, D. Seifzadeh, H. Chand, V. Krishnan, Visible-light-activated g-C_3N_4 nanosheet/carbon dot/FeOCl nanocomposites: photodegradation of dye pollutants and tetracycline hydrochloride, Colloids Surf., A, 617 (2021) 126424, doi: 10.1016/j.colsurfa.2021.126424.

[11] J. Zhang, G. Zhang, Q. Ji, H. Lan, J. Qu, H. Liu, Carbon nanodot-modified FeOCl for photo-assisted Fenton reaction featuring synergistic *in-situ* H_2O_2 production and activation, Appl. Catal., B, 266 (2020) 118665, doi: 10.1016/j.apcatb.2020.118665.

[12] X. Pan, X. Fan, A. Liang, S. Zhang, W. Wang, S. Qu, C. Li, Electron-rich CNTs modified $FeOCl/Fe_2O_3$ with improved Fenton catalytic performance, Compos. Commun., 27 (2021) 100811, doi: 10.1016/j.coco.2021.100811.

[13] M.A.N. Khan, P.K. Klu, C. Wang, W. Zhang, R. Luo, M. Zhang, J. Qi, X. Sun, L. Wang, J. Li, Metal-organic framework-derived hollow Co_3O_4/carbon as efficient catalyst for peroxymonosulfate activation, Chem. Eng. J., 363 (2019) 234–246.

[14] Y. Li, D. Chen, S. Fan, T. Yang, Enhanced visible light assisted Fenton-like degradation of dye *via* metal-doped zinc ferrite nanosphere prepared from metal-rich industrial wastewater, J. Taiwan Inst. Chem. Eng., 96 (2019) 185–192.

[15] X. Han, H. Zhang, T. Chen, M. Zhang, M. Guo, Facile synthesis of metal-doped magnesium ferrite from saprolite laterite as an effective heterogeneous Fenton-like catalyst, J. Mol. Liq., 272 (2018) 43–52.

[16] F. Liu, H. Yao, S. Sun, W. Tao, T. Wei, P. Sun, Photo-Fenton activation mechanism and antifouling performance of an FeOCl-coated ceramic membrane, Chem. Eng. J., 402 (2020) 125477, doi: 10.1016/j.cej.2020.125477.

[17] M. Nie, Y. Li, L. Li, J. He, P. Hong, K. Zhang, X. Cai, L. Kong, J. Liu, Ultrathin iron-cobalt oxide nanosheets with enhanced H_2O_2 activation performance for efficient degradation of tetracycline, Appl. Surf. Sci., 535 (2021) 147655, doi: 10.1016/j.apsusc.2020.147655.

[18] X. Shi, C. Cui, L. Zhang, J. Zhang, G. Liu, FeOCl/Ln (Ln = La or Y): efficient photo-Fenton catalysts for ibuprofen degradation, New J. Chem., 43 (2019) 16273–16280.

[19] L. Jiang, L. Zhang, C. Cui, J. Zhang, G. Liu, J. Song, Efficient degradation of phenol using Sn^{4+} doped FeOCl as photo-Fenton catalyst, Mater. Lett., 240 (2019) 30–34.

[20] S. Qu, W. Wang, X. Pan, C. Li, Improving the Fenton catalytic performance of FeOCl using an electron mediator, J. Hazard. Mater., 384 (2019) 121494, doi: 10.1016/j.jhazmat.2019.121494.

[21] D. Lu, Z. Chen, Q. Yang, S. Han, Efficient novel FeOCl/C with high singlet oxygen generation for TCH degradation, Chem. Phys. Lett., 800 (2022) 139664, doi: 10.1016/j.cplett.2022.139664.

[22] J. Wei, X. Feng, X. Hu, J. Yang, C. Yang, B. Liu, Cu(II) doped FeOCl as an efficient photo-Fenton catalyst for phenol degradation at mild pH, Colloids Surf., A 631 (2021) 127754, doi: 10.1016/j.colsurfa.2021.127754.

[23] L. Wang, H. Yang, L. Kang, M. Wu, Y. Yang, Highly dispersed of Ag/AgCl nanoparticles on exfoliated FeOCl nanosheets as photo-Fenton catalysts for pollutants degradation *via* accelerating Fe(II)/Fe(III) cycle, Chemosphere, 296 (2022) 134039, doi: 10.1016/j.chemosphere.2022.134039.

[24] W. Pei, J. Chen, D. You, Q. Zhang, M. Li, Y. Lu, Z. Fu, Y. He, Enhanced photovoltaic effect in Ca and Mn co-doped $BiFeO_3$ epitaxial thin films, Appl. Surf. Sci., 530 (2020) 147194, doi: 10.1016/j.apsusc.2020.147194.

[25] S. Guan, R. Li, X. Sun, T. Xian, H. Yang, Construction of novel ternary $Au/LaFeO_3/Cu_2O$ composite photocatalysts for RhB degradation *via* photo-Fenton catalysis, Mater. Technol., 36 (2020) 603–615.

[26] S. Qu, C. Li, X. Sun, J. Wang, H. Luo, S. Wang, J. Ta, D. Li, Enhancement of peroxymonosulfate activation and utilization efficiency *via* iron oxychloride nanosheets in visible light, Sep. Purif. Technol., 224 (2019) 132–141.

[27] E. Jara, J.A. Barreda-Argüeso, J. Gonzalez, F. Rodriguez, R. Valiente, Origin of the piezochromism in Cs_2CuCl_4: electron-phonon and crystal-structure correlations, Phys. Rev. B: Condens. Matter, 99 (2019) 134106, doi: 2469-9950/2019/99(13)/134106(9).

[28] J. Luo, M. Sun, C.L. Ritt, X. Liu, Y. Pei, J.C. Crittenden, M. Elimelech, Tuning Pb(II) adsorption from aqueous solutions on ultrathin iron oxychloride (FeOCl) nanosheets, Environ. Sci. Technol., 53 (2019) 2075–2085.

[29] Y. Zhu, R. Zhu, L. Yan, H. Fu, Y. Xi, H. Zhou, G. Zhu, J. Zhu, H. He, Visible-light Ag/AgBr/ferrihydrite catalyst with enhanced heterogeneous photo-Fenton reactivity *via* electron transfer from Ag/AgBr to ferrihydrite, Appl. Catal., B, 239 (2018) 280–289.

[30] J. Wang, Y. Li, Q. Jiang, S. Tong, Study on why FeOCl has high Fenton activity in wide range of initial pH and its corresponding stability, Process Saf. Environ. Prot., 172 (2023) 652–658.

[31] J. Chen, H. Wu, J. Liu, Y. Su, H. Li, P. Lin, Y. Chen, W. Xiao, D. Cao, Sb-doped FeOCl nanozyme-based biosensor for highly sensitive colorimetric detection of glutathione, Anal. Bioanal. Chem., 415 (2023) 1205–1219.

[32] D. Zhao, X. Liu, M. Peng, Y. Cheng, W. Zhang, L. Hu, L. Mao, Preparation of ternary composite (WS_2-FeOCl-PANI) and its performance as auxiliary electrode in electrokinetic remediation

of simulated Cr(VI) contaminated soil, J. Environ. Chem. Eng., 9 (2021) 106748, doi: 10.1016/j.jece.2021.106748.

[33] X. Liu, W. Zhang, M. Peng, G. Zhai, L. Hu, L. Mao, The role of S and Mo doping on the dissociation of water molecule on FeOCl surface: experimental and theoretical analysis, Chem. Eng. J., 426 (2021) 131353, doi: 10.1016/j.cej.2021.131353.

[34] J. Zhang, M. Yang, Y. Lian, M. Zhong, J. Sha, G. Liu, X. Zhao, S. Liu, Ce^{3+} self-doped CeO_x/FeOCl: an efficient Fenton catalyst for phenol degradation under mild conditions, Dalton Trans., 48 (2019) 3476–3485.

Supplementary information

S1. Experimental

S1.1. Characterization

The XRD pattern of 20% MnS-FeOCl is shown in Fig. S1. When the MnS mass dosage was increased to 20%, the phase composition of MnS-FeOCl composite changed (as shown in Fig. S1). Besides FeOCl, the phase of $FeCl_2$ is observed at 2θ = 15.97°, 20.67°, and 30.99°, which correspond to (−110), (020), and (111) crystal faces of $FeCl_2$ (PDF#25-1040), respectively.

The FTIR spectra of FeOCl and 5%MnS-FeOCl composites are shown in Fig. S2. The characteristic peaks around
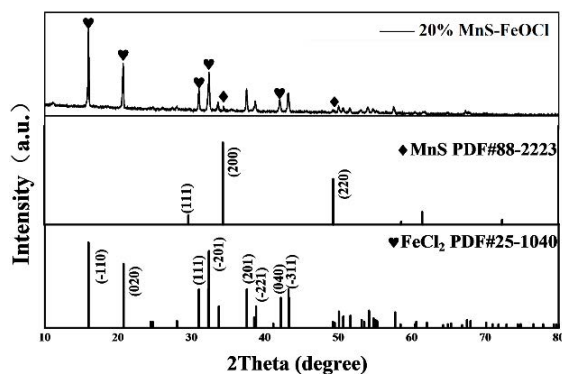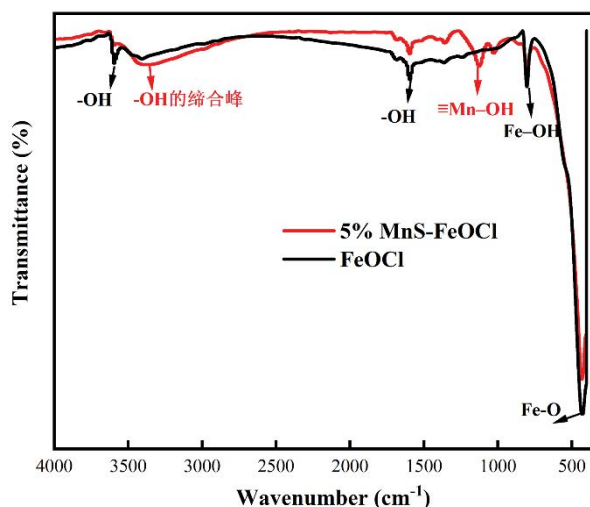
3,500 and 1,600 cm⁻¹ are the stretching vibration peak and in-plane bending vibration peak of OH group according to the IR spectral analysis. The strong and broad peak shape of the 5%MnS-FeOCl conjugated hydroxyl group in the IR results is consistent with the high percentage of hydroxyl
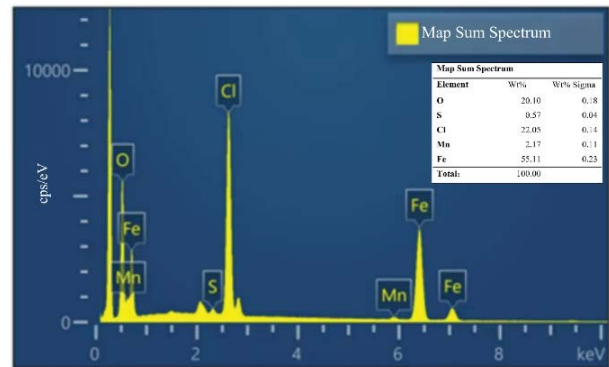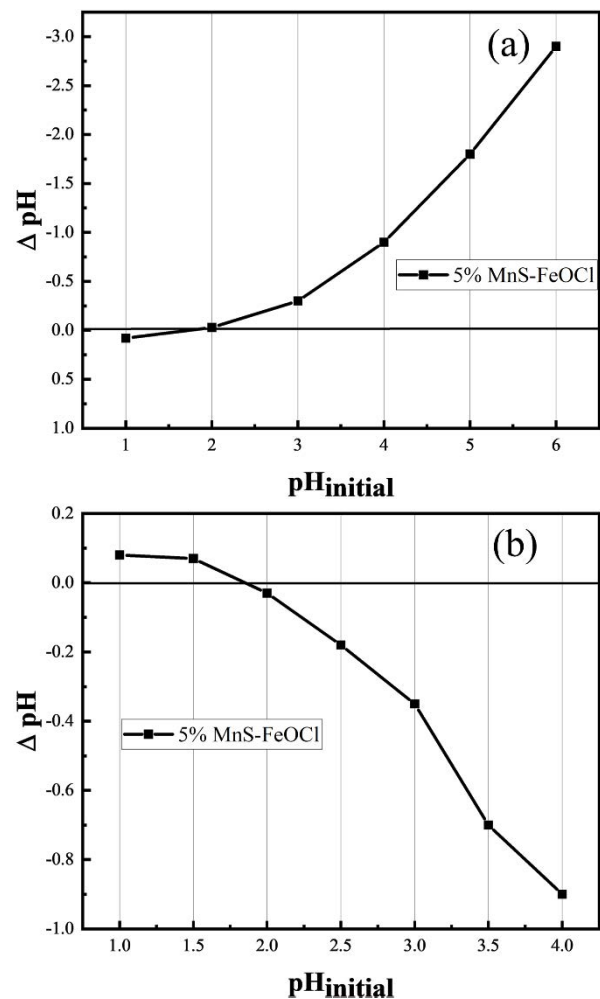

Fig. S3. Result of EDS mapping of 5% MnS-FeOCl.

Fig. S1. XRD of 20% MnS-FeOCl.

Fig. S2. FTIR of 5%MnS-FeOCl and FeOCl.

Fig. S4. pH_{PZC} measurements by the salt addition method on the large scale (a) and the small scale (b) ($\Delta pH = pH_{final} − pH_{initial}$).

oxygen content of the 5% MnS-FeOCl composite in the XPS results. 1,120 cm^{-1} is the characteristic peak of Mn–OH, 805 and 436 cm^{-1} are the characteristic peaks of Fe–OH and Fe–O, respectively.

Fig. S3 shows the EDS characterization diagram of 5% MnS-FeOCl. The results indicate that the mass ratios of Mn, S, Fe, O and Cl are 2.17%, 0.57%, 55.11%, 20.10% and 22.05%, respectively, which are close to the theoretical values.

S1.2. Measurement of pH$_{pzc}$

The pH$_{pzc}$ of 5% MnS-FeOCl composites was measured to be 1.85 (Fig. S4), which was similar to that of FeOCl. The solution pH was examined to be 4.3 within 5 min during the reaction when the initial pH was 6.0, indicating that 5%MnS-FeOCl composites also had an acidifying effect on the solution.

S1.3. Degradation of different organic

The universality of oxidative efficiency of 5%MnS-FeOCl/H$_2$O$_2$ was also tested, and *p*-aminobenzoic acid (PABA) and nicotinamide (NAM) were selected to degrade (as shown in Fig. S3). The degradation efficiencies of PABA and NAM were 63.04% and 87.53% within 5 min, respectively.

The results showed that the efficiencies of 5%MnS-FeOCl/H$_2$O$_2$ were all high in the degradation of other organic pollutants.
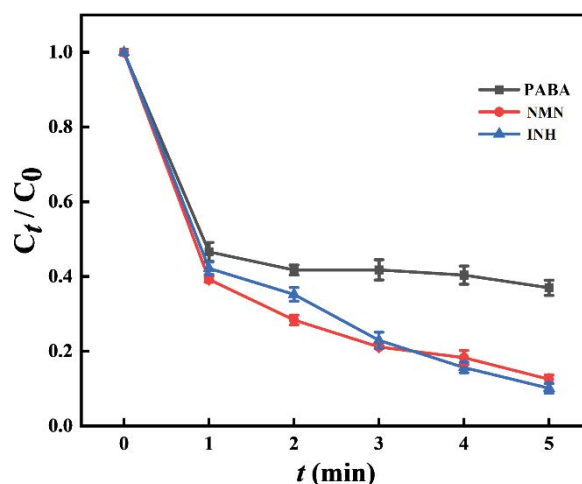

Fig. S5. Degradation of *p*-aminobenzoic acid and nicotinamide by 5%MnS-FeOCl/H$_2$O$_2$. Temperature: 25°C, catalyst dosage: 0.1 g/L, organic concentration: 20 mg/L, H$_2$O$_2$ concentration: 10 mg/L, initial pH: 6.0.